Syngeneic homograft of framework regions enhances the affinity of the mouse anti-human epidermal receptor 2 single-chain antibody e23sFv

QING OU-YANG[1,2*], JUN-LIN REN[3*], BO YAN[4*], JIAN-NAN FENG[5], AN-GANG YANG[1] and JING ZHAO[4]

[1]State Key Laboratory of Cancer Biology, Department of Immunology, Fourth Military Medical University, Xi'an, Shaanxi 710032; [2]State Key Laboratory of Kidney Diseases, Department of Nephrology, Chinese PLA General Hospital & Chinese PLA Medical School, Beijing 100853; [3]Department of Infectious Diseases, PLA Navy General Hospital, Beijing 100142; [4]Department of Biochemistry and Molecular Biology, Fourth Military Medical University, Xi'an, Shaanxi 710032; [5]Department of Immunology, Beijing Institute of Basic Medical Sciences, Beijing 100850, P.R. China

Abstract. e23sFv is a HER2-targeted single-chain variable fragment (scFV) that was characterized as the targeting portion of a HER2-targeted tumour proapoptotic molecule in our previous study. *In vitro* antibody affinity maturation is a method to enhance antibody affinity either by complementarity-determining region (CDR) mutagenesis or by framework region (FR) engraftment. In the present study, the affinity of e23sFv was enhanced using two strategies. In one approach, site-directed mutations were introduced into the FRs of e23sFv (designated EMEY), and in the other approach e23sFv FRs were substituted with FRs from the most homologous screened antibodies (designated EX1 and EX2). Notably, EX1 derived from the FR engraftment strategy demonstrated a 4-fold higher affinity for HER2 compared with e23sFv and was internalized into HER2-overexpressing cells; however, EMEY and EX2 exhibited reduced affinity for HER2 and decreased internalization potential compared with EX1. The 3D structure of EX1 and the HER2-EX1 complex was acquired using molecular homology modelling and docking and the HER2 epitopes of EX1 and the molecular interaction energy of the EX1-HER2 complex were predicted. In the present study, it was demonstrated that scFv affinity improvement based on sequence alignment was feasible and effective. Moreover, the FR grafting strategy was indicated to be more effective and simple compared with site-directed mutagenesis to improve e23sFv affinity. In conclusion, it was indicated that the affinity-improved candidate EX1 may present a great potential for the diagnosis and treatment of HER2-overexpressing tumours.

Correspondence to: Dr An-Gang Yang, State Key Laboratory of Cancer Biology, Department of Immunology, Fourth Military Medical University, 169 Changle West Road, Xi'an, Shaanxi 710032, P.R. China
E-mail: agyang@fmmu.edu.cn

Professor Jing Zhao, Department of Biochemistry and Molecular Biology, Fourth Military Medical University, 169 Changle West Road, Xi'an, Shaanxi 710032, P.R. China
E-mail: zhaojing@fmmu.edu.cn

*Contributed equally

Introduction

HER2 is a member of the human EGFR family and a well-established target for HER2-overexpressing tumour treatment (1). E23 is a monoclonal antibody derived from mice immunized with HER2-overexpressing cell components and has been indicated to specifically bind to the extracellular domain of HER2 (2). In addition, e23 was generated by fusing the variable region of the light chain (VL) with that of the heavy chain (VH) to form a single-chain variable fragment (scFv) named e23sFv (3). e23sFv has been indicated to exhibit reduced molecular weight and more efficient penetration into solid tumours compared with that of e23; therefore, it has been utilized in immunoconjugates, such as immunotoxin or immune-proapoptotic molecules, as the portion targeted to HER2 (3,4). Despite its advantages in terms of size and trafficking, e23sFv exhibits a 4-fold reduced binding affinity for HER2 compared with that of e23 or the corresponding antigen-binding fragment (Fab) (5). To achieve equivalent effectiveness, a higher dose is required for antibodies with less affinity; however, an increased dose of therapeutic antibodies can result in more intensive immunogenic reactions and possibly unexpected toxicities (6). To ensure the safety and efficacy of e23sFv-derived immuno-proapoptotic molecules in HER2-targeted tumour treatment, it is necessary to enhance the affinity of e23sFv for the HER2 extracellular domain (ECD) (5).

In vitro antibody affinity maturation enhances the antibody affinity using genetic engineering (7). Several approaches have been developed to improve the antibody affinity, the majority of which have focused on the mutagenesis of the complementarity-determining region (CDR), because CDRs are directly involved in antibody-antigen interactions (7). The crystal structure of antibody-antigen complexes has revealed that specific CDR residues of an antibody directly contact antigens and thus determine the affinity and specificity of the antibody (8). Affinity improvement *in vitro* predominantly involves inducing random mutagenesis in CDRs and screening the mutants for enhanced affinity and site-directed mutagenesis to deliberately enhance the affinity based on antibody conformation (9). In addition to CDR manipulation, the pioneering work of Foote and Winter (10) has suggested that residues in the β-sheet structure of framework regions (FRs), which support CDRs, serve critical roles in the adjustment of the loop structures of CDRs. Although these residues, which are referred to as 'Vernier zone residues', do not directly interact with the antigen, careful selection of these residues may prove essential for shaping the diversity of the structures in the primary repertoire and affinity maturation (11).

In the present study, the affinity of a single variable fragment, e23sFv, was more improved using FR engineering compared with CDR mutagenesis. The e23sFv FR was substituted with FRs from the two most homologous antibodies in the National Centre for Biotechnology Information (NCBI) protein database and two candidates named EX1 and EX2 were constructed. Another candidate was constructed by e23sFv FR residue mutation based on the sequence alignment with the variable region of the homologous antibodies. All three recombinant scFvs retained the e23sFv CDRs. The affinity assays demonstrated that EX1 exhibited the highest homology with e23sFv, thereby significantly improving its affinity for HER2, and was internalized into HER2-overexpressing cells more effectively compared with the other candidates.

Materials and methods

Framework redesign of e23sFv-based scFvs by mutagenesis and engraftment. Two strategies were used to reconstitute the FRs of e23sFv, site-directed mutagenesis and CDR grafting, both of which were based on the analysis of the e23sFv amino acid sequence homology of proteins in the NCBI database (https://blast.ncbi.nlm.nih.gov/Blast.cgi). Five VL (L1-L5) and five VH (H1-H5) sequences with the highest similarity to the VL and VH domains of e23sFv are presented in Fig. 1A, and in these candidates all FRs were aligned and comparable to that of e23sFv. Detailed information on the five VLs and five VHs selected is presented in Table I.

For the site-directed mutations, five residues in the VL and six residues in the VH sequences in the e23sFv FRs, which differed among the five domains in the homologous FRs, were replaced with the most frequently occurring amino acids in the homologous proteins (Fig. 1A), with the exception of the first S-T mutation in VL, which was not substituted to ensure that the chemical characteristics of the domains were retained. The resulting e23sFv derivative with 11 point mutations was genetically optimized with *E. coli*-preferred codons, synthesized

commercially (Beijing Augct DNA-Syn Biotechnology Co., Ltd.) and designated EMEY (Fig. 1B).

For the CDR engraftment, FR scaffolds were selected from the top two VL and VH homologous domains (Fig. 1A). The FRs of L1 (the VL of the TN1 Fab) and H1 (the VH of FabOX108) were substituted into e23sFv, giving rise to a chimaera referred to as EX1 (Fig. 1B and Table I). Another chimaera, EX2, was generated by substituting the FRs of L2 (the VL of daclizumab) and H2 (the VH of 5E1 Fab) into e23sFv (Fig. 1B and Table I). The codons of EX1 and EX2 were further optimized for prokaryotic expression and synthesized by Beijing Augct DNA-Syn Biotechnology Co., Ltd.

Prokaryotic expression and purification of the e23sFv derivatives. The genes encoding e23sFv-derived scFvs fused with His-tag at the 3' end and with 5'- and 3'-flanking *Nco*I and *Not*I restriction sites were cloned into the prokaryotic expression vector pET28a (Takara Biotechnology Co., Ltd.). The resulting recombinant plasmids were verified by agarose gel electrophoresis using 1% gel and ethidium bromide visualization. The recombinant plasmids were then transformed into *E. coli* BL21 (DE3) (Takara Biotechnology Co., Ltd.), and after 3 h of induction with 1 mM isopropyl β-d-1-thiogalactopyranoside (IPTG) at 37˚C, the bacteria were harvested and sonicated for 30 min at 2 sec intervals on ice for use in SDS-PAGE analysis to demonstrate the presence of the proteins of interest in inclusion bodies. For the purification of inclusion bodies, the precipitates were dissolved in 8 M urea buffer and subjected to Ni^{2+}-NTA affinity chromatography using Ni-NTA His•Bind Resins (Novagen; MilliporeSigma) according to the manufacturer's instructions. After extensive washing with 100 mM imidazole buffer, the bound proteins were eluted at room temperature with 1,000 mM imidazole buffer and refolded by linearly decreasing the urea gradient (7, 6, 4, 2, 1 and 0 M). The renatured proteins were finally dialyzed into PBS (pH 7.4) and quantified by BCA assay (Pierce; Thermo Fisher Scientific, Inc.).

Identification of the e23sFv derivatives by SDS-PAGE and western blotting. SDS-PAGE (12%) was performed using renatured e23sFv proteins (30 µg per sample). The protein electrophoresis gel was stained using Coomassie brilliant blue R-250 followed by greyscale analysis of the purity of the scFvs with Image J (version 1.44; National Institutes of Health). Specifically, the background-corrected density of the protein band was divided by the background-corrected density of the entire lane and multiplies by 100 to obtain the purity percentages. The e23sFv-based scFvs were identified by immunoblotting using nitrocellulose membranes. Membranes were blocked with 2% non-fat milk at room temperature for 1 h and was then incubated with anti-His antibody conjugated to horseradish peroxidase (1:1,000 dilution; cat. no. 34460; Qiagen, Inc.) at 4˚C overnight followed by chemiluminescent detection using Pierce™ ECL Western Blotting Substrate (cat. no. 32209; Thermo Fisher Scientific, Inc.) according to the manufacturer's instructions.

FITC labelling of the e23sFv derivatives. For the quantification of cellular binding and visualization of the subsequent internalization by HER2-overexpressing cells, the purified
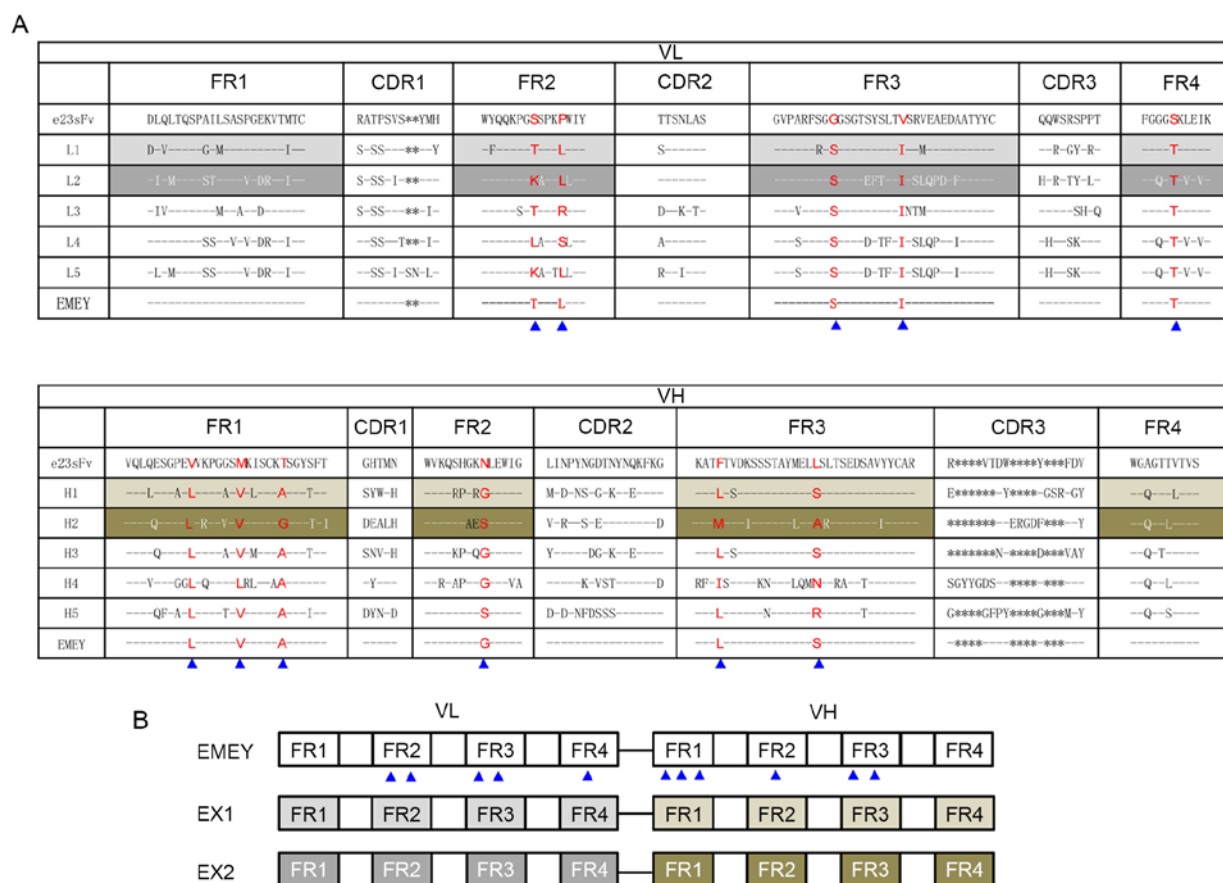
Figure 1. Design of FR-engineered e23sFv derivatives. (A) Amino acid sequence alignment of the VL and VH domains of mouse anti-HER2 single-chain variable fragment, e23sFv, and their five most homologous counterparts identified in the National Centre for Biotechnology Information protein database. L1-L5 represent VL homologous sequences and H1-H5 represent VH homologous sequences. CDRs and FRs are indicated in columns. The residues that are identical to those of e23sFv are indicated with dashed lines, and missing residues in the CDRs are indicated with asterisks. Non-identical FR residues in e23sFv and all their five homologs in the VL or VH collection are in red. Introduced site-directed mutations are indicated by blue triangles, above which are the corresponding substituted residues. (B) The schematic structure of three e23sFv derivatives. EMEY includes 11 mutated residues in the FRs of e23sFv, as indicated by triangles. EX1 and EX2 represent CDR grafts of e23sFv in the L1-H1 and L2-H2 FR scaffolds, respectively. FR, framework region; VL, light-chain variable region; VH, heavy-chain variable region; CDR, complementarity-determining region.

e23sFv-derived scFvs were conjugated with FITC using Hook™ dye labelling kit (G-Biosciences). The FITC-labelled scFvs were sterilized using 0.22 μm centrifugal filters (EMD Millipore). The absorption of fluorescein at 495 nm was detected by a UV-2450 spectrophotometer (Shimadzu Corporation), and the molar ratio of FITC to scFv was ~2.5:1.

Binding affinity to recombinant HER2 as determined by ELISA. Recombinant human HER2 (Sino Biological; 500 ng per well) was immobilized on 96-well plates at 4˚C for 16 h. The HER2-coated plates were blocked with 1% BSA (Sigma-Aldrich; Merck KGaA) at room temperature for 1 h and incubated with the three-fold-serially diluted e23sFv derivatives from 3 μM for 4 h at room temperature. ScFv15 served as the negative control. After washing with PBS-Tween-20 (0.05%; PBS-T), the bound scFvs were incubated with an HRP-conjugated anti-His antibody (1:2,000 dilution; cat. no. 34460; Qiagen, Inc.) for 1 h at room temperature. Following extensive washing with PBS-T, the microplates were incubated with a 2,2'-azino-bis (3-ethylbenzothiazoline-6-sulfonic acid) diammonium salt (7 mM) substrate at 37˚C for 20 min, and the absorbance was measured at 409 nm using a Sunrise microplate reader (Tecan Group, Ltd.).

Measurement of the affinity constant by surface plasmon resonance (SPR). An SPR assay was used for the kinetic analysis of the binding of the e23sFv-based scFvs to recombinant HER2 *in vitro*. A ProteOn™ GLC sensor chip (Bio-Rad Laboratories, Inc.) was immobilized with 5 μg/ml HER2 in 10 mM acetate (pH 5.5). Five solutions in PBS-T with two-fold serial dilutions of the e23sFv derivatives were injected and run through the sensor chip at a flow rate of 50 μl/min. The analyte injection programme included a 180 sec association phase followed by a 600 sec dissociation phase. The data were analysed in a 1:1 Langmuir binding model (12) using ProteOn Manager software (Bio-Rad Laboratories, Inc.). The equilibrium constant (K_D) was calculated as the ratio of the dissociation rate constant (K_{off}) to the association rate constant (K_{on}).

Binding affinity for cellular HER2 as determined by flow cytometry. HER2-positive cells (BT-474 and SKOV-3 cells) and HER2-negative cells (MCF-7 cells) were purchased from American Type Culture Collection and cultured in RPMI-1640 medium (cat. no. 10-040-CV; Corning, Inc.) with 10% FBS (cat. no. 10099; Gibco; Thermo Fisher Scientific, Inc.) at 37˚C and 5% CO_2. After blocking in 5% BSA (cat. no. A1933; Sigma-Aldrich; Merck KGaA) at 4˚C

Table I. Detailed information of selected framework region scaffolds by homologous analysis.

Chain	Name	Origin	Entry ID	(Refs.)
L1	Chain L, human thrombopoietin neutralizing antibody TN1 Fab	*Mus musculus*	pdb|2ZKH|	16
L2	Chain B, crystal structure of the Fab fragment of therapeutic antibody daclizumab	*Mus musculus*	pdb|3NFP|	17
L3	Chain A, Fab fragment of the engineered human monoclonal antibody A5B7	*Mus musculus*	pdb|1AD0|	18
L4	Immunoglobulin H23 light chain kappa variable region	Humanized	gb|AAB38288.1|	19
L5	Chain L, structure of CD40L in complex with the Fab fragment of the humanized 5C8 antibody	Humanized	pdb|1I9R|	20
H1	Chain B, crystal structure of FabOX108	*Mus musculus*	pdb|3DGG|	21
H2	Crystal structure of sonic hedgehog bound to the 5E1 Fab fragment	*Mus musculus*	pdb|3MXW|	22
H3	Chain B, crystal structure of IL-23 in complex with neutralizing Fab	*Mus musculus*	pdb|3D85|	23
H4	Immunoglobulin heavy chain V region humanized bispecific antibody	Humanized	gb|AAB24133.1|	24
H5	Immunoglobulin heavy chain V region precursor	*Homo sapiens*	pir|PN0444|	25

Fab, antigen-binding fragment.

for 30 min, 1×10^6 HER2-positive cells (BT-474 and SKOV-3 cells) and HER2-negative cells (MCF-7 cells) were incubated with 125 nM FITC-conjugated e23sFv derivatives on ice for 1 h. For the negative control, a non-specific scFv, scFv15 against hepatitis B virus surface antigen (HbsAg), which was purified and labelled with FITC as previously described, was used at 125 nM to exclude nonspecific binding (13). In addition, a FITC-labelled anti-HER2 antibody (1:2,000; cat. no. 10004-R511-F; Sino Biological) was used as a positive control. After antibody incubation at 4˚C for 30 min, the cells were rinsed with PBS, and FITC intensities were quantified using a FACSCalibur flow cytometer (BD Biosciences) with CellQuest software (BD Biosciences).

Internalization as assessed by fluorescence microscopy. HER2-positive cells (BT-474 and SKOV-3 cells) and HER2-negative cells (MCF-7 cells) were cultured on coverslips (1×10^6 cells/well in a six-well plate). After blocking in 5% BSA (cat. no. A1933; Sigma Aldrich; Merck KGaA) at 4˚C for 30 min, cells were incubated with 500 nM FITC-labelled e23sFv derivatives at 37˚C for 4 h. scFv15 (500 nM) was included as a negative control, which was prepared and coupled with FITC as previously described (13). After incubation, the samples were fixed in 4% paraformaldehyde at 4˚C for 30 min. Bright-field and fluorescence images of cells were captured using a fluorescence microscope (IX-71; Olympus Corporation).

Molecular modelling of mutant scFvs. The parental e23sFv and mutated variants were generated using the web-based antibody modelling software BLASTP (https://blast.ncbi.nlm.nih.gov/Blast.cgi?PAGE=Proteins), which is based on a modified form of the algorithm used for antibody modelling. We used the 'dead-end elimination' algorithm (14) for side chain building. We compared both the heavy and light chains independently with the most homologous antibodies based on the homologous protein structures obtained from the Protein Data Bank (PDB) (https://www.rcsb.org/) using the Homology module in Discovery Studio 4.5 software (BIOVIA; Dassault Systèmes). The predicted structures of e23sFv and EX1 were subsequently docked to the crystal structure of the human HER2 ECD using ZDOCK Server (http://zdock.umassmed.edu.).

Statistical analysis. All assays were performed in triplicate on three independent occasions unless otherwise stated. The data are presented as the mean ± SD. ANOVA followed by Tukey's post hoc test was used for the statistical analyses, which were performed with SPSS v15.0 software (SPSS, Inc.). $P < 0.05$ was considered to indicate a statistically significant difference.

Results

Framework engineering of e23sFv and prokaryotic expression of the e23sFv derivatives. To maintain the HER2-binding activity of e23sFv, all CDRs were maintained intact and only the FRs in the VL and VH domains were manipulated. For the purpose of FR manipulation, homologous sequences of e23sFv were selected by browsing the NCBI protein database (Fig. 1A and Table I). Two FR engineering methods were employed based on this homologous candidate list.

Firstly, site-directed mutagenesis was performed to modulate the FRs of e23sFv with as few mutations as possible and therefore only 11 amino acids, which were not identical to any of the homologous repertoires identified in the NCBI database, were replaced with the most frequently occurring residues (Fig. 1A). The mutated e23sFv derivatives harboured an 11-residue substitution, which was named EMEY (Fig. 1B). Secondly, CDR grafting of e23sFv to FR scaffolds of the two most homologous mouse VL and VH domains was
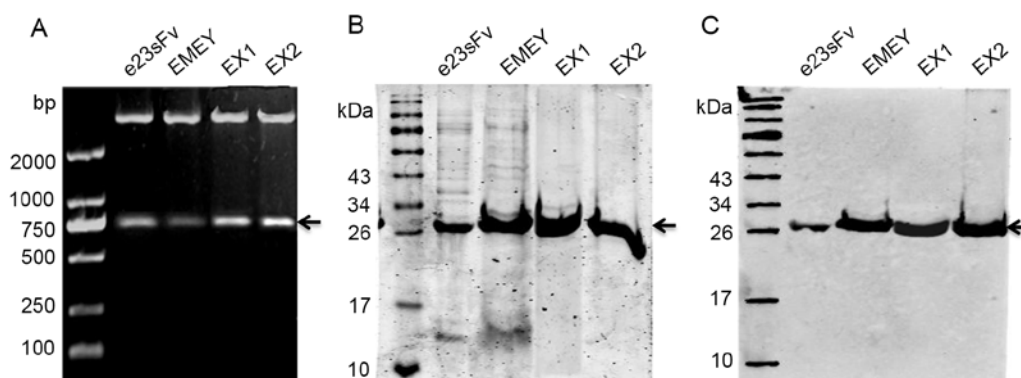
Figure 2. Prokaryotic expression and purification of the e23sFv-derived scFvs. (A) Identification of the insertion of the e23sFv-based scFv genes into the pET28a prokaryotic expression plasmid by double digestion with *Nco*I and *Not*I. Arrows indicate the bands of e23sFv and its derivatives. (B and C) Expression and purification of the e23sFv derivatives in *E. coli* BL21 (DE3). The purified e23sFv derivatives were verified by (B) SDS-PAGE and (C) western blotting with an anti-His antibody as indicated by arrows. scFv, single-chain variable fragment.

performed to avoid the risk of structurally interfering with antibody-antigen recognition. e23sFv was engrafted with L1-H1 and L2-H2 as FR acceptors, and these constructs were referred to as EX1 and EX2, respectively (Fig. 1B).

These three His-tagged-FR-engineered e23sFv-based scFv genes were cloned into a pET28a prokaryotic expression plasmid (Fig. 2A), followed by transformation into *E. coli* BL21 (DE3). IPTG induction resulted in a robust expression of the engineered scFvs in the inclusion bodies of the bacteria, which were denatured and purified by Ni^{2+}-NTA affinity chromatography. The yield of the refolded scFvs was 1 mg/l for e23sFv and 3-4 mg/l for the three derivatives, as quantified by a BCA assay, suggesting improved protein production presumably due to FR engineering. The purity of both e23sFv and EMEY was approximately 93%, as quantified by SDS-PAGE, slightly less than the 98% purity of EX1 and EX2, which indicated a subtle difference in nickel-binding dynamics resulting from the FR substitutions (Fig. 2B). All purified scFvs were confirmed by western blotting with an anti-His antibody (Fig. 2C).

In vitro binding affinity of the FR-engineered anti-HER2 scFvs. Since all the original CDRs of e23sFv were maintained intact in the three FR-engineered scFvs, their HER2-binding activities were theoretically expected to be retained. To address this hypothesis, *in vitro* ELISA was performed to detect the binding capacities of the e23sFv derivatives to recombinant HER2 that was immobilized on the microplates. As illustrated in Fig. 3A, EMEY and EX1 exhibited binding patterns similar to that of parental e23sFv, but in contrast to e23sFv, they did not reach binding saturation at the highest dose. By contrast, the binding curve of EX2 indicated that the maximal binding level of EX2 was only 68.2% compared with e23sFv, suggesting the considerably decreased ability of EX2 to bind HER2.

To further dissect the association and dissociation properties of the e23sFv-derived scFvs with recombinant HER2, SPR was performed to monitor the binding kinetics based on five sensorgrams in which different concentrations of scFvs run through a HER2-coated sensor chip. An increase in the SPR signal was observed in the nanomolar range for EX1 and e23sFv, differing from the micromolar range obtained for EMEY and EX2 (Fig. 3B). The K_D of EX1 was ~0.9 nM, exhibiting nearly a 3-fold increased binding affinity compared with that of e23sFv, with a

K_D of 2.5 nM (Fig. 3C). Given that the K_{on} of EX1 was only ~0.6-fold higher compared with that of e23sFv, the enhanced affinity of EX1 was mainly attributed to a ~4.3-fold lower K_{off}. The binding capabilities of the other two scFvs, EMEY and EX2, were diminished with a K_D value of ~0.5 and ~0.1 μM, respectively (Fig. 3C). These results indicated that EX1, when bound to recombinant HER2, exhibited a slightly faster on-rate and a slower off-rate compared with those of parental e23sFv, resulting in a stronger antibody-antigen interaction.

Cellular binding and internalization of the FR-engineered anti-HER2 scFvs. Subsequently, the potential of the e23sFv derivatives to recognize endogenous HER2 was evaluated. Three cell lines with differential HER2 expression levels were incubated with FITC-labelled e23sFv derivatives, and the percentages of the bound cells were quantified by flow cytometry. As demonstrated in Fig. 4, in the BT-474 breast cancer cells that express high levels of HER2 (~100% in the case of the positive binding control), EX1 bound to >90% of the cell population, comparable to the binding capacity of e23sFv, whereas the cellular binding of EMEY and EX2 decreased to less than 30% of the cell population. Similar results were observed in the SKOV-3 ovarian cancer cells with moderate HER2 expression, demonstrating comparable binding activities between EX1 and e23sFv and impaired binding of EMEY and EX2. Fluorescent HER2-negative MCF-7 breast cancer cells were undetected, as was the non-specific HbsAg-targeting scFv15, indicating the specificity of this cell-based binding assay.

It was also determined whether interaction with cell surface HER2 enabled the e23sFv derivatives to enter the cells. Intracellular fluorescence of the FITC-labelled e23sFv derivatives was monitored in HER2-positive cell lines 4 h post-incubation. In contrast to the negative controls consisting of MCF-7 cells and scFv15, a patchy distribution of EX1 fluorescence was observed in both BT-474 and SKOV-3 cells, indicating endosomal localization similar to the pattern of e23sFv (Fig. 5). However, the fluorescence of the other two variants was faint compared with that of e23sFv and EX1, which indicated a weaker HER2 binding and internalization.

Docking mechanism of the enhanced EX1-HER2 interaction. The *in silico* docking analysis revealed that both e23sFv and
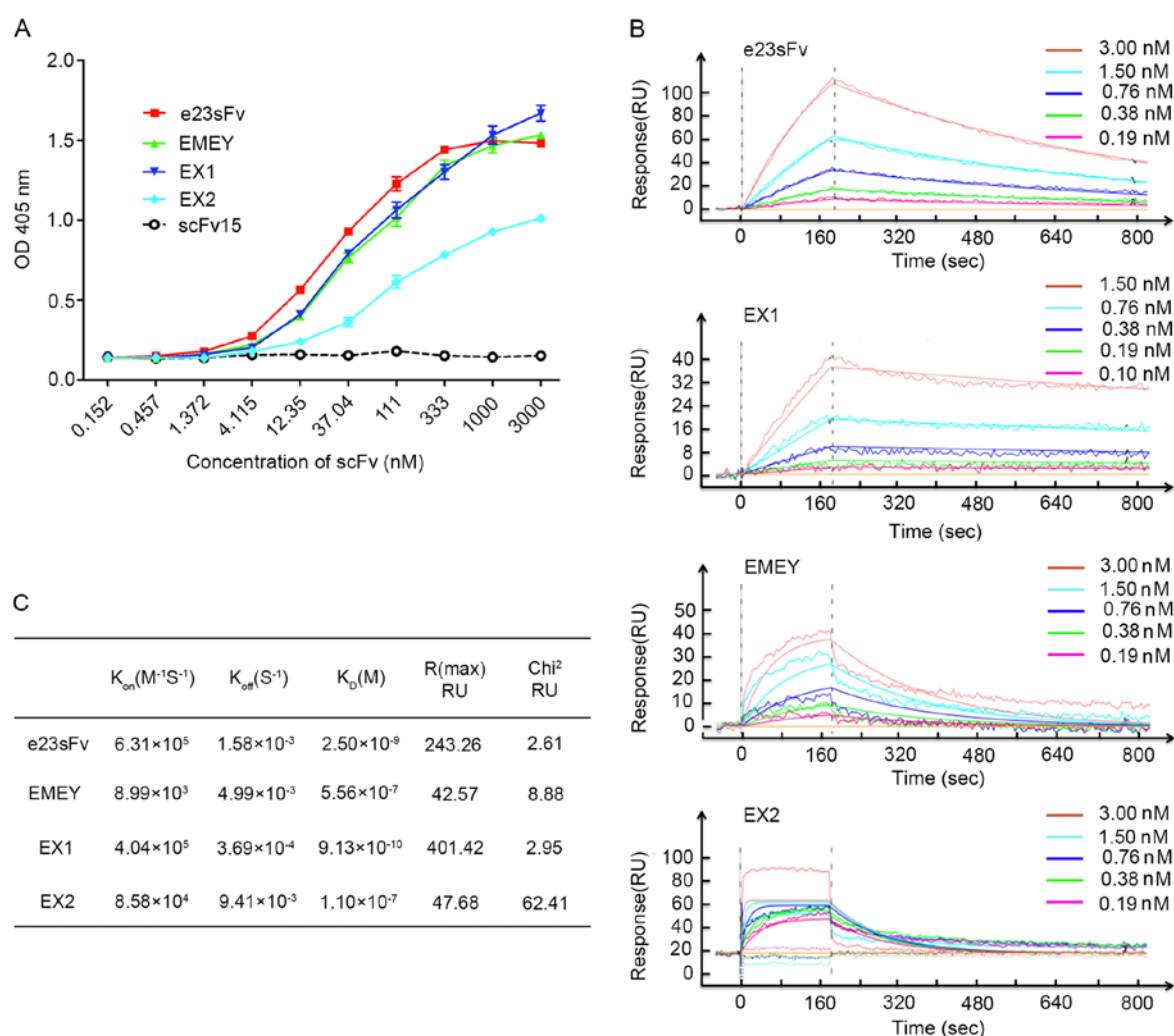
Figure 3. *In vitro* binding of the e23sFv-derived scFvs to recombinant HER2. (A) Affinity measurement by ELISA. HER2-coated microplates were incubated with the e23sFv derivatives at various concentrations, and the bound scFvs were detected using an anti-His antibody. scFv15 served as the negative control. (B) One-shot kinetics of SPR. Five sensorgrams indicated the response of HER2-immobilized sensor chips with five diluted concentrations of the e23sFv derivatives. (C) Comparison of K_{on}, K_{off} and K_D of the e23sFv derivatives calculated from SPR sensing. scFv, single-chain variable fragment; SPR, surface plasmon resonance; RU, resonance unit; K_{on}, association rate constant; K_{off}, dissociation rate constant, K_D, equilibrium constant; Chi², goodness-of-fit between the binding model and theoretical affinity; OD, optical density.

the three mutants bound to domain IV of the HER2 ECD, and several residues were identified as putatively important for these binding interfaces (Fig. 6A-D). All the scFv variants formed distinct but overlapping interfaces with domain IV of the HER2 ECD (Fig. 6E). The HER2 binding energy of EX1 was predicted to be slightly higher compared with that of e23sFv while EMEY and EX2 showed decreased binding energy compared with e23sFv (Fig. 6E).

Discussion

e23sFv is an scFv derived from the HER2-targeted monoclonal antibody e23 by fusing its VL with its VF (3). e23sFv exhibits a decreased molecular size compared with its IgG counterpart e23 and can therefore penetrate solid tumours more effectively (3). However, e23sFv has been indicated to exhibit a decreased affinity for HER2 by a factor of 4 compared with that of e23 or the corresponding e23 Fab, according to the results of a competitive binding assay (4). With a decreased affinity, the function of e23sFv as the targeting moiety has

been lessened (4). Therefore, improving the affinity of e23sFv is of great importance to maintain the targeting function of e23sFv. The decreased affinity of e23sFv compared with that of e23 has been primarily attributed to conformational alterations after its reconstruction (4). Restoration of the affinity of e23sFv may be effectively accomplished by mutagenesis approaches to manipulate the interface of antibody-antigen contact.

CDRs in the antibody variable region are well-known as the antibody repertoire-determining regions and are responsible for antigen-antibody interactions (7,8). Hotspots of somatic mutations during the process of antibody affinity maturation are predominantly located in CDRs, which indicates that the diversity of the amino acids in CDRs mainly accounts for antibody specificity and affinity (7,8). Based on the critical role that CDRs serve in antigen binding, mutations are frequently introduced into CDRs to obtain high affinity variants in the practice of *in vitro* antibody affinity improvement (15). However, β-sheets in the FRs of the antibody variable region serve a scaffold role for the loop structure of
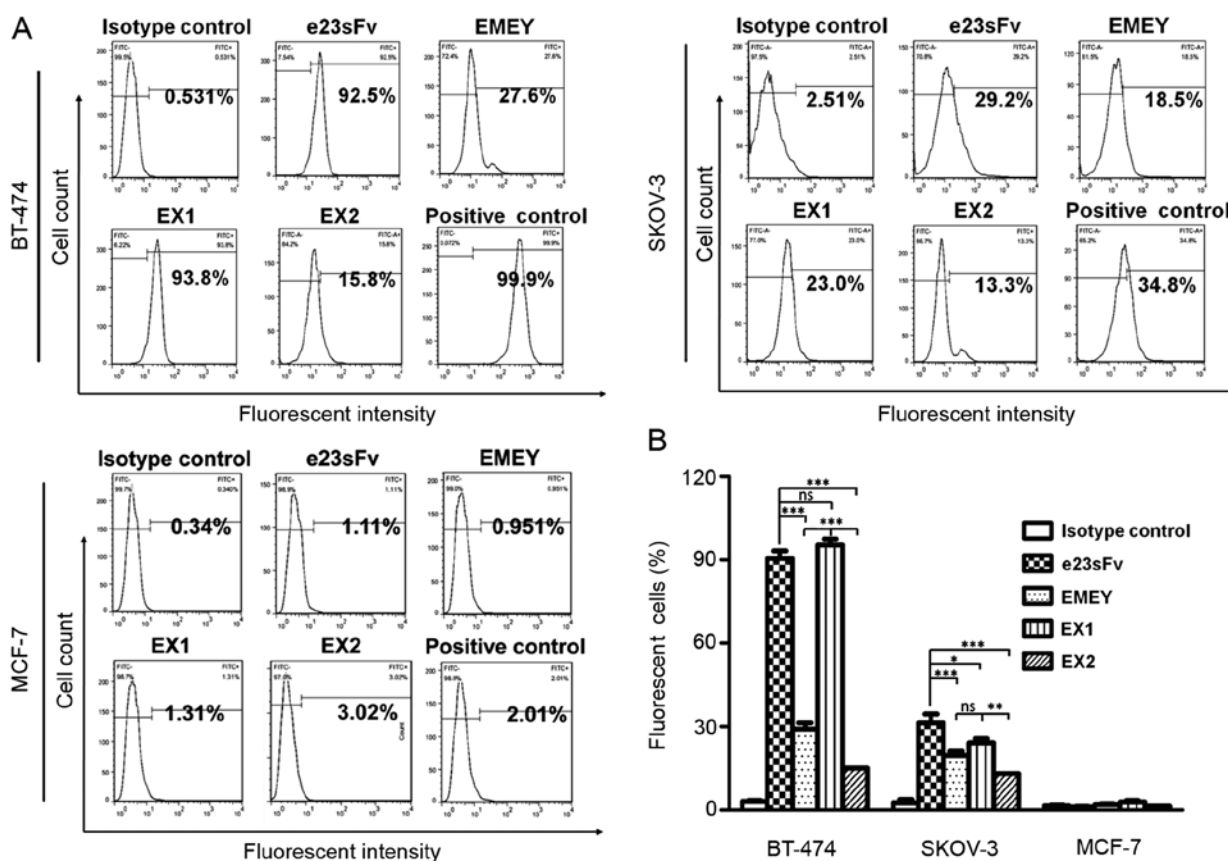
Figure 4. Binding of the e23sFv-derived single-chain variable fragments to HER2 on the cell surface. HER2-positive cells (BT-474 and SKOV-3 cells) and HER2-negative cells (MCF-7 cells) were incubated with FITC-labelled e23sFv derivatives and subjected to flow cytometry analysis. (A) Representative dataset of one-parameter histograms. For the isotype control, FITC-labelled scFv15 against HBsAg was used. For the positive control, a commercial FITC-conjugated anti-HER2 antibody was used. (B) Statistical analysis from three independent parallel experiments. *P<0.05; **P<0.01 and ***P<0.001. ns, non-significant.

the CDRs, and specific residues in the FRs supporting the CDR loops can affect loop folding and fine-tune their binding to antigens (10). Furthermore, FR residues in the periphery of CDRs have been indicated to be in direct contact with antigens (16). Consequently, FR engineering may serve as an alternative approach to improve antibody affinity by modulating the antibody-antigen interface with no risk of losing binding specificity. The present study used FR grafting to improve the affinity of the scFv of e23sFv, which has been indicated to bind HER2 with superior specificity in previous studies (3). Firstly, NCBI was searched for antibody variable region sequences homologous with the VL and VH of e23sFv. Subsequently, the FRs in e23sFv were replaced with the corresponding segments from the top two homologous sequences to generate two engrafted scFvs, named EX1 and EX2.

The mutagenesis of the residues in the CDRs or FRs, ranging from site-directed to undirected randomized mutations is based on the conformational information of the antibody and high-throughput screening procedures to obtain affinity-improved antibodies (17). In the present study, an affinity-improved antibody, EX1, was obtained by transplanting the FRs of the homologous antibody heavy and light chains into e23sFv. The affinity of EX1 was improved by a factor of 3 compared with that of e23sFv according to the SPR assay, and this reconstruction was based on the absence of any conformational information. Sequence alignment indicated that the residue similarity of the Vernier zone of FRs in

the e23sFv and the candidates determined the extent of the affinity improvement. EMEY, which exhibited a ~200-fold decreased affinity for HER2 compared with that of e23sFv in the SPR assay, carried one mutation (G64S) in the Vernier zone of VL and one mutation (F69L) in that of VH compared with e23sFv. EX1, which exhibited a three-fold increased affinity for HER2 compared with that of e23sFv, carried two additional mutations (L2V and Y35F) in the VL Vernier zone and four additional mutations (Q2K, S27T, F69L and V71S) in the VH Vernier zone. For comparison with EMEY, EX1 was constructed by substituting the FRs of e23sFv with counterparts from the top sequence based on homology (18,19). The SPR binding assay demonstrated that EX1 exhibited 3-fold increased affinity for recombinant human HER2 compared with that of e23sFv, with an increased K_{on} value and decreased K_{off} value. In the binding assay performed with flow cytometry, EX1 exhibited higher affinity for HER2-overexpressing cell lines compared with that of parental e23sFv. The *in silico* docking analysis indicated that e23sFv and the three mutants bound to domain IV of the HER2 ECD, with several residues putatively important for establishing binding interfaces. The binding energy of HER2 with EX1 was predicted to be slightly higher compared with that of e23sFv. The docking analysis also revealed that all the scFvs formed distinct but overlapping interfaces with domain IV of the HER2 ECD, which indicated that the manipulation of the FRs mildly influenced the binding specificity of the scFvs.
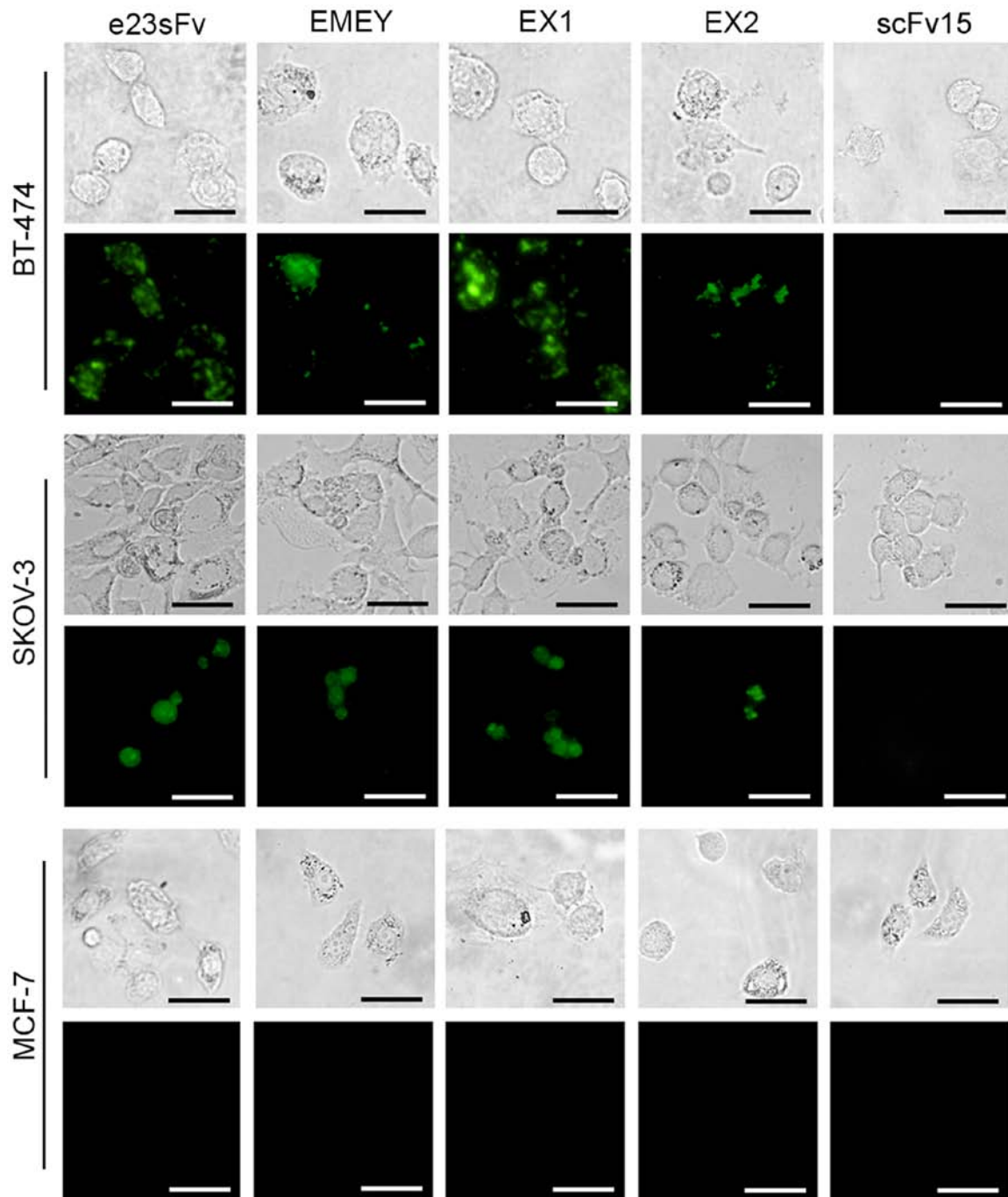
Figure 5. Internalization of the e23sFv-derived single-chain variable fragments by HER2-positive cells. Following incubation with FITC-labelled e23sFv derivatives, BT-474, SKOV-3 and MCF-7 cells were observed under fluorescence microscopy. MCF-7 cells served as the HER2-negative cell controls and scFv15 was the non-specific binding control. Scale bar, 100 μm. The data are representative of at least three independent experiments.

A potent application of scFvs in tumour diagnosis and treatment requires the administration of scFvs at a dose sufficient for tumour targeting with minimal off-tumour effects (5). The improved affinity of EX1 for efficient HER2 binding required a small dose, which indicated that it poses a reduced risk of off-target effects and is less likely to induce toxicity in organs, such as the liver and kidney. Moreover, a small dose may result in less intense immunogenic reactions and lower costs for treatment, which are also important issues to consider. Immunofluorescence experiments indicated that EX1 can be internalized into cells after binding to HER2 on the cell surface, which may suggest that proapoptotic molecules, such as tBid,

or caspase-6 among others, can be fused to the C-terminus of EX1 as in our previous studies, and be internalized with scFv into tumour cells (4). The internalized molecules are presumed to enter endosomes with HER2 molecules and be carried and released to kill tumour cells, which guarantees the success of subsequently applied antibody-based therapeutics. The internalized proapoptotic molecules are subsequently translocated to the cytoplasm where they execute proapoptotic activity. The construction of an EX1-proapoptotic fusion protein and analysis of its antitumour toxicity are ongoing projects.

The approach of the present study for *in vitro* antibody maturation was based on protein sequence alignment and domain
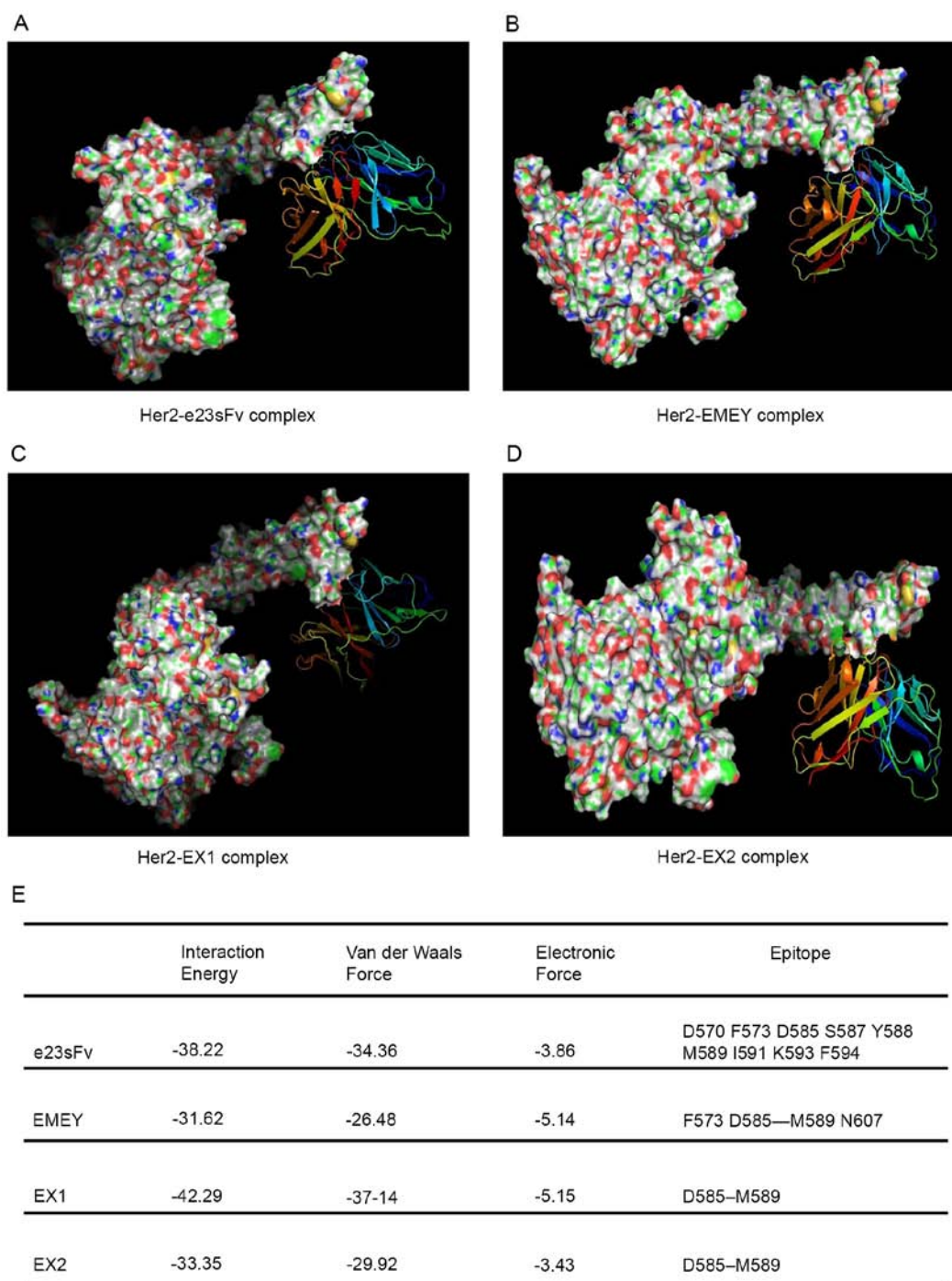
Figure 6. Docking mechanism of the enhanced EX1-HER2 interaction. (A-D) *In silico* docking of e23sFv, EMEY, EX1 and EX2 and their interactions with the predicted surface models of the HER2 ECD. All the scFv fragments form distinct but overlapping interfaces with domain IV of the HER2 ECD. The 3D structures of (A) e23sFv, (B) EMEY, (C) EX1 and (D) EX2 are presented as coloured ribbons. (E) Binding energy with HER2 and the predicted binding epitopes of all the scFv fragments. ECD, extracellular domain; scFv, single-chain variable fragment.

grafting. Affinity-improved candidates were achieved by retaining the CDRs of the parental scFv and substituting the FRs with the counterparts from a homologous antibody. This approach maintained the conformational structure of the parental scFv and the maximal binding specificity to the antigen. Moreover, FR grafting is more straightforward compared with site-directed mutagenesis at specific residues because the mutations are frequently based on the crystal structure of the antigen-antibody complex (7). However, several candidates in the present study were indicated to exhibit a partially decreased affinity for HER2 compared with e23sFv. One plausible explanation may be that the alterations in FR core residues failed to fully contribute to antibody folding and resulted in functional loss. Nonetheless, the methodology used in the current study was indicated to be of satisfactory efficiency and can be widely applied for antibody affinity improvement. In conclusion, the FR grafting strategy was indicated to be more effective and simple compared with site-directed mutagenesis to improve e23sFv affinity. Moreover, it was indicated that the affinity-improved candidate EX1 may be used for the diagnosis and treatment of HER2-overexpressing tumours.

Availability of data and materials

The datasets used and/or analysed during the current study are not publicly available because they are part of an ongoing project but are available from the corresponding author on reasonable request.

Authors' contributions

JLR, JZ and AGY designed the research. QOY and BY performed all the experiments. JNF performed the molecular modelling analysis. JZ and AGY wrote the manuscript. All author read and approved the final manuscript.

Ethics approval and consent to participate

Not applicable.

Patient consent for publication

Not applicable.

Competing interests

The authors declare that they have no competing interests.

References

1. Rimawi MF, Schiff R and Osborne CK: Targeting HER2 for the Treatment of Breast Cancer. Annu Rev Med 66: 111-128, 2015.
2. Kasprzyk PG, Song SU, Di Fiore PP and King CR: Therapy of an animal model of human gastric cancer using a combination of anti-erbB-2 monoclonal antibodies. Cancer Res 52: 2771-2776, 1992.
3. Batra JK, Kasprzyk PG, Bird RE, Pastan I and King CR: Recombinant anti-erbB2 immunotoxins containing Pseudomonas exotoxin. Proc Natl Acad Sci USA 89: 5867-5871, 1992.
4. Jia LT, Zhang LH, Yu CJ, Zhao J, Xu YM, Gui JH, Jin M, Ji ZL, Wen WH, Wang CJ, *et al*: Specific tumoricidal activity of a secreted proapoptotic protein consisting of HER2 antibody and constitutively active caspase-3. Cancer Res 63: 3257-3262, 2003.
5. Ou-Yang Q, Yan B, Li A, Hu ZS, Feng JN, Lun XX, Zhang MM, Zhang MD, Wu KC, Xue FF, *et al*: Construction of humanized anti-HER2 single-chain variable fragments (husFvs) and achievement of potent tumor suppression with the reconstituted husFv-Fdt-tBid immunoapoptotin. Biomaterials 178: 170-182, 2018.
6. Mazor R, Onda M and Pastan I: Immunogenicity of therapeutic recombinant immunotoxins. Immunol Rev 270: 152-164, 2016.
7. Sheedy C, Mackenzie CR and Hall JC: Isolation and affinity maturation of hapten-specific antibodies. Biotechnol Adv 25: 333-352, 2007.
8. Briney B, Sok D, Jardine JG, Kulp DW, Skog P, Menis S, Jacak R, Kalyuzhniy O, de Val N, Sesterhenn F, *et al*: Tailored immunogens direct affinity maturation toward HIV neutralizing. Cell 166: 1459-1464.e11, 2016.
9. Prassler J, Steidl S and Urlinger S: In vitro affinity maturation of HuCAL antibodies: Complementarity determining region exchange and RapMAT technology. Immunotherapy 1: 571-583, 2009.
10. Foote J and Winter G: Antibody framework residues affecting the conformation of the hypervariable loops. J Mol Biol 224: 487-499, 1992.
11. Teplyakov A, Obmolova G, Malia TJ, Raghunathan G, Martinez C, Fransson J, Edwards W, Connor J, Husovsky M, Beck H, *et al*: Structural insights into humanization of anti-tissue factor antibody 10H10. MAbs 10: 269-277, 2018.
12. Zhang L, Cai QY, Cai ZX, Fang Y, Zheng CS, Wang LL, Lin S, Chen DX and Peng J: Interactions of bovine serum albumin with anti-cancer compounds using a ProteOn XPR36 array biosensor and molecular docking. Molecules 21: 1706, 2016.
13. Yan B, Ouyang Q, Zhao Z, Cao F, Wang T, Jia X, Meng Y, Jiang S, Liu J, Chen R, *et al*: Potent killing of HBV-related hepatocellular carcinoma by a chimeric protein of anti-HBsAg single-chain antibody and truncated Bid. Biomaterials 34: 4880-4889, 2013.
14. LuCore SD, Litman JM, Powers KT, Gao S, Lynn AM, Tollefson WT, Fenn TD, Washington MJ and Schnieders MJ: Dead-end elimination with a polarizable force field repacks PCNA structures. Biophys J 109: 816-826, 2015.
15. Tiller KE, Chowdhury R, Li T, Ludwig SD, Sen S, Henry KA and Tessier PM: Facile affinity maturation of antibody variable domains using natural diversity mutagenesis. Front Immunol 8: 986, 2017.
16. Chothia C and Lesk AM: Canonical structures for the hypervariable regions of immunoglobulins. J Mol Biol 196: 901-917, 1987.
17. Moreira GMSG, Fuhner V and Hust M: Epitope mapping by phage display. Methods Mol Biol 1701: 497-518, 2018.
18. Tahara T, Kuwaki T, Matsumoto A, Morita H, Watarai H, Inagaki Y, Ohashi H, Ogami K, Miyazaki H and Kato T: Neutralization of biological activity and inhibition of receptor binding by antibodies against human thrombopoietin. Stem Cells 16: 54-60, 1998.
19. Wright GJ, Cherwinski H, Foster-Cuevas M, Brooke G, Puklavec MJ, Bigler M, Song Y, Jenmalm M, Gorman D, McClanahan T, *et al*: Characterization of the CD200 receptor family in mice and humans and their interactions with CD200. J Immunol 171: 3034-3046, 2013.